Research Square

Preprints are preliminary reports that have not undergone peer review.
They should not be considered conclusive, used to inform clinical practice,
or referenced by the media as validated information.

# A Dive Into The Spatial Patterns of the Endosymbionts of Actinostella spp. (Cnidaria, Actiniaria, Actiniidae) via Genome-Skimming, Metabarcoding and Transcriptomics

**Jeferson A. Durán-Fuentes**
Universidade Estadual Paulista (Unesp)
**Júlia M. Molina**
Universidade Estadual Paulista (Unesp)
**Thais B. Santos**
Universidade Estadual Paulista (Unesp)
**Marymegan Daly**
The Ohio State University
**Adam Reitzel**
University of North Carolina at Charlotte
**Eulalia Peraza**
Universidad de La Laguna
**Emilio Lanna**
Universidade Federal da Bahia
**James D. Reimer**
University of the Ryukyus
**Sergio N. Stampar**
sergio.stampar@unesp.br

Universidade Estadual Paulista (Unesp)

**Research Article**

**Keywords:** Actiniaria, biogeography, ITS2 metabarcoding, Symbiodiniaceae, SymPortal, Western South Atlantic

**Posted Date:** November 26th, 2026

**DOI:** https://doi.org/10.21203/rs.3.rs-10846325/v1

**License:** This work is licensed under a Creative Commons Attribution 4.0 International License. Read Full License

**Additional Declarations:** No competing interests reported.

## Abstract

Symbiodiniaceae associations in sea anemones can vary across host species, geographic regions, and individual hosts, but the factors underlying this variation remain poorly understood. Here, we investigated the diversity and geographic structure of Symbiodiniaceae associated with Tropical Atlantic Ocean populations of *Actinostella* spp. by integrating internal transcribed space 2 (ITS2) metabarcoding analysed through the SymPortal framework with complementary genome-skimming and transcriptomic datasets. ITS2 metabarcoding of Brazilian populations revealed high-resolution variation in symbiont composition between tropical and subtropical regions, whereas genome-skimming and transcriptomic data expanded the detection of Symbiodiniaceae lineages across multiple *Actinostella* species and geographic localities. The combined datasets revealed associations with three Symbiodiniaceae genera: *Breviolum*, *Symbiodinium*, and *Cladocopium*. *Breviolum* was consistently recovered from metabarcoded specimens and represented a widespread component across host populations, with shared ITS2 profiles connecting tropical Northeast (NE) and subtropical Southeast Brazil (SE). In contrast, *Symbiodinium* showed a stronger association with tropical populations, whereas *Cladocopium* exhibited heterogeneous occurrence among individuals and regions. Fine-scale ITS2 profiling revealed substantial variation among individual sea anemones from the same locality, indicating that *Actinostella* populations collectively harbour a diverse Symbiodiniaceae repertoire rather than a single fixed host–symbiont association. These findings expand the understanding of non-scleractinian cnidarian–Symbiodiniaceae relationships and highlight *Actinostella* as a valuable model for investigating the ecological and evolutionary mechanisms shaping symbiont diversity across tropical and subtropical environments.


## INTRODUCTION

Together, the clades Operculozoa (Medusozoa and Endocnidozoa) and Anthozoa (Ceriantharia, Hexacorallia, and Octocorallia), both belonging to Cnidaria,constitute one of the most diversified animal group in terms of life cycle, ecology, and morphology (DeBiasse et al. 2024; Zapata et al. 2015). Sea anemones, anthozoans of the order Actiniaria, are strictly polypoid cnidarians widely distributed across marine habitats, spanning broad latitudinal and bathymetric gradients where environmental factors, particularly temperature, together with substrate availability and, for some species, salinity, influence their occurrence and distribution (Daly et al. 2008; Fautin et al. 2013; Rodríguez et al. 2014; Sun et al. 2021; Targino and Gomes 2020). Beyond their well-recognised role as benthic predators (Morejón-Arrojo et al. 2025), actiniarians contribute to the primary production of coastal ecosystems through obligate or facultative associations with photosynthetic endosymbionts, particularly dinoflagellates of the family Symbiodiniaceae (LaJeunesse et al. 2018; Murray et al. 2016; Parkinson et al. 2025).

Symbiodiniaceae Fensome, Taylor, Norris, Sarjeant, Wharton & Williams, 1993 currently comprises 12 valid genera (Guiry and Guiry 2026; LaJeunesse et al. 2018; Parkinson et al. 2025) with *Symbiodinium* LaJeunesse, 2017 (former Clade A), *Breviolum* Parkinson & LaJeunesse, 2018 (Clade B) and *Cladocopium* LaJeunesse & H.J. Jeong, 2018 (Clade C) being the genera most frequently recovered from cnidarian hosts in the Atlantic (Bell and Quigley 2025). Symbiont taxonomic identity has profound functional consequences for the symbiotic relationship: a proteomic and metabolomic study of the model anemone *Exaiptasia diaphana* showed that hosting *Breviolum minutum*, *Symbiodinium linucheae*, or *Durusdinium trenchii* triggered markedly different responses to thermal stress, with no single symbiont conferring superior tolerance across all metrics (Lust et al. 2025). Symbiont identity also modulates lipid signalling, nitrogen exchange and host fitness across generations (Botana 2025; Crehan 2025; McCauley et al. 2025), reinforcing the view that fine-scale resolution of the symbiont community is essential to understanding the holobiont performance.

Although most literature on Symbiodiniaceae-cnidarian symbioses still focuses on reef-building scleractinian corals, a growing body of work shows that non-scleractinian hosts harbour symbiont communities with distinct compositions. A comparative survey of unicellular hosts (e.g., Foraminifera and Ciliophora), multicellular hosts (e.g., Actiniaria, Scleractinia, Scyphozoa and Tridacninae), and environmental reservoirs concluded that anemones (Actiniaria) and

jellyfish (Scyphozoa) frequently associate with symbiont lineages that are rare or absent in sympatric scleractinian corals, suggesting partly independent symbiont pools across host groups (Emelianenko et al. 2026). Likewise, a recent global analysis of coral-associated protists highlighted that sea anemones, zoantharians and corallimorpharians harbor Symbiodiniaceae assemblages structurally distinct from those of scleractinians, implying that conclusions drawn from scleractinian corals should not be transposed uncritically to other anthozoans (del Campo et al. 2026). At local scales, microhabitat-level studies of intertidal anemones have demonstrated that even within a single host species, the dominant symbiont strain can vary across the vertical zonation gradient (Ruggeri et al. 2024), providing a mechanistic basis for the spatial heterogeneity reported in actiniarian holobionts (Clerissi et al. 2026; Sydnor et al. 2023).

The intensifying pressure of climate change has made the study of non-scleractinian coral cnidarian holobionts especially timely. The marine heatwaves of 2022–2024 caused near-complete local extinctions of host anemones and their fish in parts of the Red Sea (Bennett-Smith et al. 2025) and have left persistent legacy effects on Symbiodiniaceae assemblages that can outlast the bleaching event itself (Buzzoni et al. 2026; Cavailles et al. 2025). In this context, sea anemones are increasingly seen as tractable model systems for understanding the limits of cnidarian symbiotic flexibility (Anthony et al. 2025; Beauson 2025; Gamache 2025; Glass 2025; Moya-Hernández and Moya 2026). Two proposed and complementary mechanisms underlie this flexibility: *shuffling*, the change in the relative abundance of symbiont lineages already present in the host (Baker 2003; Buddemeier and Fautin 1993; Cavailles et al. 2025; MacVittie et al. 2024), and *switching*, the acquisition of new symbionts from the environment (Crehan 2025; Davies et al. 2023; Parkinson et al. 2025). Both processes depend on the size and composition of the host's symbiont repertoire, a dimension that is not straightforwardly predicted by the host's geographic range, since a widely distributed host may associate with a narrow set of symbiont lineages, and a geographically restricted host may harbour a surprisingly diverse symbiont assemblage. The relationship between host biogeography and symbiont repertoire breadth is therefore not one of simple correspondence, but rather an empirical question in its own right and one that remains poorly resolved for most non-coral hosts of the western South Atlantic.

The focus of this study comprises 43 specimens of three lineages of sea anemones of the genus *Actinostella* Duchassaing, 1850 from across the Atlantic Ocean. Two are currently considered valid species (Durán-Fuentes et al. 2026). Among them, *A. flosculifera* (Le Sueur, 1817) is the most extensively studied and exhibits the widest reported distribution, ranging from Cuba and other localities in the Caribbean Sea and Gulf of Mexico to the southern Brazilian coast (Barragán et al. 2024; Durán-Fuentes et al. 2022, 2023, 2026; González-Muñoz et al. 2012, 2013; Herrera-Bojórquez et al. 2020). *Actinostella yucatanensis* Durán-Fuentes, González-Muñoz, Lizaola-Guillermo & Stampar, 2026 was recently described from Chabihau Beach, on the Yucatán Peninsula, Mexico (Durán-Fuentes et al. 2026). Populations from the Canary Islands in the Eastern Atlantic are referred to herein as *Actinostella* sp., based on morphological differences from *A. flosculifera* (see Durán-Fuentes et al. 2026).

Species of *Actinostella* possess a distinctive morphological structure called a marginal ruff, composed of frond-like marginal projections of both endo- and exo-coels. The marginal ruff is conspicuously enriched with Symbiodiniaceae (Barragán et al. 2024; Durán-Fuentes et al. 2026). Despite the broad distribution of the genus *Actinostella* across tropical and subtropical regions of the Atlantic Ocean, the diversity and biogeographic structure of its associated Symbiodiniaceae remain poorly understood, and no broad-scale comparison has yet evaluated how Symbiodiniaceae communities vary among and within *Actinostella* populations across the Atlantic.

Here, we investigate Symbiodiniaceae diversity associated with *Actinostella* specimens collected from across a broad geographic range encompassing populations from Florida (US), Mexico, Colombia, Brazil, and the Canary Islands (Spain). Given the inherent logistical challenges of standardizing broad-scale sampling for these understudied anemones, we adopted an integrative, opportunistic approach. We leveraged targeted nuclear ribosomal internal transcribed spacer 2 (ITS2) metabarcoding (analyzed through the SymPortal framework; Hume et al. 2019) alongside non-target Symbiodiniaceae sequences mined from newly generated transcriptomic and genome-skimming datasets. While this

integration yields an asymmetrical sampling design, it serves as a powerful proof-of-concept for repurposing diverse high-throughput sequencing data to assess symbiont diversity and geographic variation at multiple levels of resolution.

Specifically, we aimed to: (i) characterise the taxonomic diversity and composition of Symbiodiniaceae associated with *Actinostella* spp. across the Atlantic; (ii) evaluate geographic variation in symbiont assemblages among populations spanning tropical and subtropical regions; (iii) compare patterns of Symbiodiniaceae diversity recovered using ITS2 metabarcoding, transcriptomic, and genome-skimming datasets; and (iv) assess whether symbiont associations exhibit geographic structuring across the sampled range or reveal patterns potentially associated with host identity and regional environmental conditions.

# MATERIALS AND METHODS

# Metabarcoding approach

# Study sites and specimen collection

Specimens of *Actinostella flosculifera* (n = 7) were collected from rocky intertidal habitats during spring low tides at two localities along the Brazilian coast, spanning approximately 10.5° of latitude and representing two distinct biogeographic provinces of the western South Atlantic (Fig. 1). Three individuals were collected at Praia da Pituba, Salvador, Bahia, northeastern Brazil (SBA, 12°59'51"S, 38°26'31"W), within the Tropical Brazilian Province, on September 20, 2025. An additional four individuals were collected at Praia do Codó (Prainha), Ubatuba, São Paulo, southeastern Brazil (USP, 23°30'04"S, 45°07'08"W), located within the Subtropical Paulista Province, on August 15, 2025.

All specimens were sampled at a maximum depth of ~ 1 m at low tide. Individuals were carefully detached from the substrate using stainless-steel forceps, photographed in situ, and immediately preserved in absolute ethanol (99.6%) at ambient temperature for transport. Voucher specimens were subsequently deposited in the Laboratory of Evolution and Aquatic Diversity (LEDA Lab), São Paulo State University (UNESP), and stored at − 20°C until DNA extraction.

## DNA extraction, ITS2 amplicon library preparation and sequencing

Total genomic DNA was extracted from approximately 1 cm² of tissue excised from the margin of the marginal ruff of each specimen. Extractions were carried out in a Class II laminar-flow cabinet using a silica-column extraction kit (Quatro G Biotecnologia, ref. 100197) following the manufacturer's protocol, with negative controls included in each batch. The quantity and purity (A260/A280 and A260/A230 ratios) of the recovered DNA were assessed on a NanoDrop spectrophotometer.

The internal transcribed spacer 2 (ITS2) region of the nuclear ribosomal DNA is the standard marker for Symbiodiniaceae profiling (LaJeunesse 2002; LaJeunesse et al. 2018) and was PCR-amplified using the primer pair ITSint-for2 (forward, 5'-GAATTGCAGAACTCCGTG-3'; LaJeunesse and Trench 2000) and ITS2rev (reverse, 5'-GGGATCCATATGCTTAAGTTCAGCGGG-3'; Coleman et al. 1994). Library preparation, indexing and paired-end sequencing (2 × 300 bp) were performed by an external service provider on an Illumina NextSeq 2000 platform. Demultiplexed forward (R1) and reverse (R2) .fastq.gz files were retrieved for downstream processing, with file integrity verified through SHA-256 hashes (recorded in the sample-metadata table).

## Bioinformatic processing, read pre-processing and quality control

ITS2 sequence data were submitted to the SymPortal analytical framework (Hume et al. 2019; SymPortal.org), which performs quality control, Symbiodiniaceae-specific taxonomic assignment and ITS2 *type-profile* resolution through identification of Defining Intragenomic Variants (DIVs) rather than fixed similarity clustering. The full pipeline based on wrapped around mothur v1.39.5 (Schloss et al. 2009), the BLAST+ suite (Camacho et al. 2009), Minimum Entropy Decomposition (MED; Eren et al. 2015) and custom Python modules was executed with default parameters as detailed below. Paired-end reads were assembled into contigs in mothur with the make.contigs command. Forward and reverse primer regions were trimmed using pcr.seqs (pdiffs = 2, rdiffs = 2). Contigs were then filtered with screen.seqs (maxambig = 0, maxhomop = 5), and only sequences between 184 bp and 310 bp in length were retained. Singletons and doubletons were removed with split.abund (cutoff = 2). The number of raw contigs and quality-controlled sequences per sample is reported in the SymPortal output table under the columns *raw_contigs*, *post_qc_absolute_seqs* and *post_qc_unique_seqs*.

## Symbiodiniaceae-specific taxonomic assignment

Quality-controlled sequences were classified taxonomically by blastn (max_target_seqs = 1) against the SymPortal-curated reference database, which contains representative ITS2 sequences for the nine Symbiodiniaceae genera (former clades A through I, corresponding to the genera *Symbiodinium*, *Breviolum*, *Cladocopium*, *Durusdinium*, *Effrenium*, *Fugacium*, *Gerakladium*, *Halluxium* and *Freudenthalidium*-related lineages *sensu* LaJeunesse et al. 2018). Sequences not matching a Symbiodiniaceae reference (e.g. host-derived, prey-derived or environmental contaminant DNA) were partitioned into the *post_taxa_id_absolute_non_symbiodiniaceae_seqs* fraction and excluded from further symbiont-community analyses. Sequences shorter or longer than the expected size range or showing unrealistic length distributions were tagged as *size_screening_violation* and discarded.

# Minimum Entropy Decomposition (MED)

To consolidate biologically meaningful sequence variants and minimise the impact of PCR/sequencing artefacts, the Symbiodiniaceae-only sequence set was processed by Minimum Entropy Decomposition (MED; Eren et al. 2015), which discriminates sequence variants on the basis of informative (high-entropy) nucleotide positions rather than overall similarity thresholds. The output of this step was recorded in the *post_med_absolute* (total reads) and *post_med_unique* (unique sequences) columns of the sample-metadata table.

## Genus-level community composition

The 27 ITS2 sequence variants (see Results, below) were aggregated at the genus level using the clade-to-genus correspondence established by LaJeunesse et al. (2018): Clade A → *Symbiodinium*; Clade B → *Breviolum*; Clade C → *Cladocopium*. Relative abundances per genus per sample were computed by summing absolute post-MED read counts of all ITS2 variants belonging to the same clade and dividing by the total Symbiodiniaceae read count for that sample. The "*noName Clade A–I*" output columns, which captured clade-level signals that could not be assigned to a named profile, contained no reads in the present dataset and confirmed that all Symbiodiniaceae sequences were resolved at the DIV level with no unassigned clade-level residual.

# Downstream analyses and visualisation

The genus-level relative-abundance matrix was tabulated for the seven specimens (Table 1) and visualised as a 100%-stacked bar chart using Python v3.11 with the pandas v2.2 and matplotlib v3.8 libraries. ITS2 richness per specimen was estimated as the number of distinct ITS2 profiles with non-zero relative abundance recovered after MED. Biogeographic differences in community composition were inspected by direct comparison of genus-level proportions and of the

dominant DIV(s) per sample, with no inferential statistical testing applied because of the limited number of biological replicates per site (N = 3 in SBA, N = 4 in USP); the present study is therefore reported as an exploratory characterisation of the *A. flosculifera* — Symbiodiniaceae system in the western South Atlantic. Sample-level community dissimilarity was computed as the Bray–Curtis index from the full 7 × 27 post-MED relative-abundance matrix. The resulting dissimilarity matrix was used to build a sample-level UPGMA dendrogram (scipy.cluster.hierarchy.linkage, method = 'average') displayed alongside the abundance heatmap in Fig. 2.

Table 1
Genus-level composition of Symbiodiniaceae (post-MED relative abundance, %) of *Actinostella flosculifera*, based on metabarcoding approach. ITS2 profiles = number of DIV-resolved type profiles with non-zero abundance per sample.

| Localities | Sample | *Symbiodinium* (A) | *Breviolum* (B) | *Cladocopium* (C) | Total ITS2 profiles |
|---|---|---|---|---|---|
| Salvador, Bahia (SBA) | SBA-1 | 37.13 | 62.87 | 0.00 | 14 |
| | SBA-2 | 24.12 | 38.19 | 37.69 | 16 |
| | SBA-3 | 38.58 | 61.42 | 0.00 | 14 |
| Ubatuba, São Paulo (USP) | USP-1 | 0.00 | 100.00 | 0.00 | 4 |
| | USP-5 | 0.00 | 100.00 | 0.00 | 4 |
| | USP-9 | 0.00 | 100.00 | 0.00 | 4 |
| | USP-10 | 0.00 | 64.26 | 35.74 | 5 |

# Genome-skimming and transcriptomic approaches

## Study sites and sample collection

Twenty-eight individuals of *Actinostella flosculifera* were collected from multiple localities across the Atlantic Ocean (Fig. 1): one specimen from Cabo Frio, Rio de Janeiro, Brazil (CF-Br; 22°57'27"S, 42°00'59"W); five from Ubatuba, São Paulo, Brazil (UB-Br; 23°30'04"S, 45°07'09"W); five from Ipojuca, Pernambuco, Brazil (MA-Br; 8°25'44"S, 34°58'35"W); one from Florianópolis, Santa Catarina, Brazil (FSC-Br; 27°46'58.3"S, 48°30'25"W); one from Punta Bello, Córdoba, Colombia (PB-Co; 9°25'10.7"N, 75°44'32.4"W); and fifteen from Niles Road Beach, Summerland Key, Florida, USA (NSK; 24°41'11.4"N, 81°26'38.3"W). Additionally, for this analysis, five individuals of *A. yucatanensis* were included: four from Chabihau, Yucatán, Mexico (YU-Me; 21°21'25"N, 89°07'36"W) and one from Tavernier, Florida, USA (FLK; 25°01'18.8"N, 80°30'49.1"W). Finally, three specimens provisionally identified as *Actinostella* sp. were included from the Canary Islands, Spain (CI-SP; 28°07'43"N, 15°27'10"W).

Voucher specimens were deposited in the Museum of Zoology of the University of São Paulo, Brazil (MZUSP), and the Instituto de Investigaciones Marinas y Costeras “José Benito Vives de Andréis” (INVEMAR) (registration code: MZUSP 8734–8747 and INV-CNI-4810, respectively) (Table 1).

## DNA extraction and genome-skimming sequencing

Twenty individuals representing the CF-Br, CI-SP, FSC-Br, MA-Br, PB-Co, UB-Br, and YU-Me populations were processed using a genome-skimming approach. Small tissue fragments (~ 25 mg) from the pedal disc were excised and preserved in absolute ethanol for molecular analyses. Genomic DNA was extracted using the QIAamp DNA Blood Kit (Qiagen) from these twenty samples. DNA input for library preparation ranged from 364 to 1,744 ng. Library preparation and sequencing were performed at the University of Wisconsin–Madison Collaborative Genomics Core using an Illumina NovaSeq X Plus platform with 150 bp paired-end reads.

## RNA extraction and transcriptome sequencing

Fifteen individuals from NSK were assayed as part of the transcriptomic study by Durán-Fuentes et al. (under revision), which evaluated thermal stress responses in marginal ruff and tentacles of *A. flosculifera*. For the present study, only transcriptomic data derived from marginal ruff tissue were analyzed. Transcriptomic data from the FLK specimen were also included, with analyses based on marginal ruff tissue.

Marginal ruff tissues were dissected and preserved in RNAlater™ (Thermo Fisher Scientific) at 4°C until RNA extraction for RNA-seq analysis at the University of North Carolina at Charlotte. For RNA extraction, the RNeasy® Plus Micro Kit (Qiagen) was used. Between 30 and 50 mg of tissue were homogenized in 350 µL of Buffer RLT Plus using a syringe and transferred to a gDNA Eliminator spin column following the manufacturer's protocol. RNA quantity was measured using a Qubit® Flex Fluorometer and a Qubit™ RNA BR Assay Kit, and quality was assessed using a TapeStation (Agilent Technologies, USA).

All samples showed an RNA Integrity Number (RIN) ≥ 7.1 (range: 7.1–8.8), and RNA concentrations were quantified using Qubit fluorometry, ranging from 71.8 to 646 ng/µL. For library preparation, RNA input was normalized to 250 ng of total RNA per sample. Sixteen RNA libraries were generated from 250 ng of total RNA using the NEBNext® UltraExpress RNA Library Prep kit, NEBNext® Poly(A) mRNA Magnetic Isolation Module, and NEBNext® Multiplex Oligos for Illumina (New England Biolabs), and sequenced as 2 × 150 bp paired-end reads on an Illumina NovaSeq™ 6000 platform (Illumina, USA).

# ITS2 capture bioinformatic workflow

Raw FASTQ files were quality-filtered and trimmed using Fastp v0.23.4 (Chen 2025). Reads previously identified as belonging to Symbiodiniaceae were mapped using BWA-MEM v2.3 (Li and Durbin 2009) against clade-specific reference sequences corresponding to complete ribosomal regions of Symbiodiniaceae, including representatives of distinct ITS2 lineages (Supplementary Table S1).

Resulting alignments were sorted and indexed using SAMtools v1.23.1 (Danecek et al. 2021) and mapping statistics were summarized using the flagstat module. Mapped reads were subsequently extracted from BAM alignments and converted back into FASTQ format using SAMtools. These ITS2-enriched read sets were assembled independently for each specimen. Genome-skimming reads were assembled using SPAdes v4.3.0 (Bankevich et al. 2012) in --only-assembler mode with a single-end configuration, whereas transcriptomic reads were assembled using Trinity v2.15.2 (Grabherr et al. 2011) with default parameters.

Final assemblies were imported into Geneious Prime 2024.0, where contigs corresponding to the ITS2 region were manually inspected and curated for each specimen. ITS2 sequences were then individually extracted and retained for downstream analyses of Symbiodiniaceae diversity and comparisons among host individuals.

# Phylogenetic analyses

The ITS2 sequences recovered through metabarcoding, genome-skimming, and transcriptomic approaches were analyzed together with reference Symbiodiniaceae ITS2 sequences retrieved from GenBank (Supplementary Table S1), including sequences generated by Nitschke et al. (2020), Parkinson et al. (2015), and Pochon et al. (2012). *Pelagodinium beii* and *Protodinium simplex* (GenBank accessions: JN558106 and JN558103, respectively) were used as outgroups (Supplementary Table S1). The sequences of all taxa were imported into Geneious Prime 2024.0 and mapped against the ITS2 dataset generated in the present study to delimit homologous boundaries and retain only the ITS2 region, avoiding the inclusion of adjacent ribosomal markers.

Sequences were aligned using MAFFT v7.53 with the L-INS-i algorithm and the "--maxiterate 1000" option (Supplementary Material S2; Katoh and Standley 2013). Maximum-likelihood (ML) phylogenetic reconstruction was conducted using IQ-TREE 2 (Minh et al. 2020). The best-fitting nucleotide substitution model (TPM2u + F+I+G4) was selected according to the Bayesian Information Criterion (BIC) using ModelFinder (Kalyaanamoorthy et al. 2017), as implemented in IQ-TREE 2.

Branch support was assessed using 1,000 SH-like approximate likelihood ratio test (SH-aLRT) replicates and 1,000 ultrafast bootstrap (UFBoot2) replicates (Hoang et al. 2018) (Supplementary Material S3). The resulting tree was edited and visualized using TreeGraph 2 (Stöver and Müller 2010).

## RESULTS

# Metabarcoding approach

# Overall sequencing output and Symbiodiniaceae recovery

ITS2 amplicon sequencing of the seven *A. flosculifera* specimens, SymPortal pre-processing (mothur 1.39.5 + BLAST+) and Minimum Entropy Decomposition (MED) yielded between $6.0 \times 10^{15}$ and $3.1 \times 10^{16}$ post-MED paired-end reads per sample (sample UIDs 267840–267846; data-set 20260327T192550_stampse1). Across the seven specimens, there were 10 unique post-MED sequences and zero reads assigned to the "*noName Clade A–I*" residual columns, confirming that all Symbiodiniaceae sequences were resolved at the DIV (Defining Intragenomic Variant) level with no unassigned clade-level signals. Host-derived (*Actinostella flosculifera*) and exogenous eukaryotic sequences (macroalgae, neighbouring cnidarians) were partitioned into the *post_taxa_id_absolute_non_symbiodiniaceae_seqs* fraction and excluded from the symbiont analyses.

# Genus-level community composition

The metabarcoding pipeline resolved 27 distinct ITS2 profiles distributed across three Symbiodiniaceae genera — *Symbiodinium* (8 profiles), *Breviolum* (12 profiles) and *Cladocopium* (7 profiles). No reads matched *Durusdinium*, *Effrenium*, *Fugacium*, *Gerakladium* or any other Symbiodiniaceae genus (Fig. 2 and Table 1). *Breviolum* was the only genus recovered in all host specimens (relative abundance 38.2–100%). *Symbiodinium* was strictly restricted to the Northeast of Brazil (SBA-1, SBA-2 and SBA-3; 24.1–38.6% of reads) and entirely absent from the Southeast (Table 1). *Cladocopium* displayed an intermediate distribution, appearing as a substantial component (> 35%) in one specimen per region and undetected in the remaining five specimens (Fig. 2 and Table 1).

# ITS2 profile richness and biogeographic partitioning

Specimens from SBA hosted 3–4x more ITS2 profiles than those from USP (mean ± SD: 14.7 ± 1.2 vs 4.3 ± 0.5 profiles per sample). Sub-generic structure (Table 2) revealed a strong partition of ITS2 profiles between regions. All eight *Symbiodinium* profiles were SBA-exclusive, and seven of the twelve *Breviolum* profiles were also restricted to SBA (90033_B, 30054_B, 6699874_B, 29222_B, 89438_B, 29334_B and 6699875_B), whereas the remaining five *Breviolum* profiles (B1, B14a, B1au, B1g and 29445_B) were shared between regions. Within *Cladocopium*, six of the seven profiles recovered (C1, C42.2, C1b, C42ao, 5429_C and 11808_C) were SBA-exclusive and entirely restricted to specimen SBA-2, whereas C3 was USP-exclusive and accounted, in isolation, for all the *Cladocopium* signal detected in USP-10.

Table 2

ITS2 type profiles recovered in *Actinostella flosculifera* (SymPortal output). Frequencies indicate the number of specimens (out of 3 SBA and 4 USP) in which the profile was detected. Profiles in **bold** in the "Distribution" column are part of the *Breviolum* backbone shared across both regions. Localities– SBA: Salvador, Bahia; USP: Ubatuba, São Paulo.

| Genus / Clade | ITS2 profile | SBA freq. (/3) | USP freq. (/4) | Distribution | Max. relative abundance (sample) |
|---|---|---|---|---|---|
| **Symbiodinium** (A) | A4 | 3 | 0 | SBA-exclusive | 6.55% (SBA-3) |
| | A4ax | 3 | 0 | SBA-exclusive | 13.04% (SBA-2) |
| | 285996_A | 3 | 0 | SBA-exclusive | 26.55% (SBA-1) |
| | 6699873_A | 3 | 0 | SBA-exclusive | 4.76% (SBA-3) |
| | 38158_A | 2 | 0 | SBA-exclusive | 5% (SBA-3) |
| | 30702_A | 1 | 0 | SBA-exclusive | 5.32% (SBA-3) |
| | 136585_A | 1 | 0 | SBA-exclusive | 5.26% (SBA-3) |
| | 136341_A | 1 | 0 | SBA-exclusive | 4.03% (SBA-3) |
| **Breviolum** (B) | **B1** | 3 | 4 | **Shared / core** | **22.8%** (USP-1) |
| | **B14a** | 3 | 4 | **Shared / core** | **25.93%** (USP-9) |
| | **B1au** | 2 | 2 | **Shared / core** | **65.6%** (USP-5) |
| | **B1g** | 3 | 4 | **Shared / core** | **19.85%** (USP-9 / USP-1) |
| | **29445_B** | 2 | 2 | **Shared / core** | **34.01%** (USP-1) |
| | 90033_B | 2 | 0 | SBA-exclusive | 14.84% (SBA-3) |
| | 30054_B | 1 | 0 | SBA-exclusive | 7.98% (SBA-2) |
| | 6699874_B | 1 | 0 | SBA-exclusive | 0.79% (SBA-2) |
| | 29222_B | 1 | 0 | SBA-exclusive | 6.56% (SBA-1) |
| | 89438_B | 1 | 0 | SBA-exclusive | 5.05% (SBA-1) |
| | 29334_B | 1 | 0 | SBA-exclusive | 8.23% (SBA-3) |
| | 6699875_B | 1 | 0 | SBA-exclusive | 4.14% (SBA-1) |
| **Cladocopium** (C) | C1 | 1 | 0 | SBA-exclusive | 20.06% (SBA-2) |
| | C42.2 | 1 | 0 | SBA-exclusive | 1.61% (SBA-2) |

| Genus / Clade | ITS2 profile | SBA freq. (/3) | USP freq. (/4) | Distribution | Max. relative abundance (sample) |
|---|---|---|---|---|---|
| | C1b | 1 | 0 | SBA-exclusive | 9.39% (SBA-2) |
| | C42ao | 1 | 0 | SBA-exclusive | 6.34% (SBA-2) |
| | 5429_C | 1 | 0 | SBA-exclusive | 0.29% (SBA-2) |
| | 11808_C | 1 | 0 | SBA-exclusive | < 0.01% (SBA-2) |
| | C3 | 0 | 1 | USP-exclusive | 35.74% (USP-10) |

Within *Symbiodinium*, which was confined to SBA, the most abundant DIVs were 285996_A (up to 26.6% in SBA-1) and A4ax (up to 13.0% in SBA-2), with SBA-3 standing out as the specimen with the highest *Symbiodinium* richness (8 profiles) and therefore the most diverse *Symbiodinium* sub-community. Within *Breviolum*, present at both regions, four core profiles — B1, B14a, B1au and B1g — were recovered in almost every specimen, but dominance shifted at the sub-generic level: B1au dominated USP-5 (65.6%), 29445_B dominated USP-1 (34.0%) and USP-9 (33.7%), and B14a peaked in USP-9 (25.9%), whereas in SBA no single *Breviolum* profile exceeded 20%, indicating a more even distribution of the genus across multiple co-occurring DIVs in the tropical Northeast Brazil. The two specimens with substantial *Cladocopium* signal differed sharply at the sub-generic level: SBA-2 hosted a C1-/C1b-dominated sub-community supplemented by five further co-occurring *Cladocopium* profiles, whereas USP-10 hosted an exclusively C3-typed *Cladocopium*, a profile completely absent from SBA.

# Genome-skimming and transcriptomic approaches

# DNA- and RNA-seq Data Quality and Processing

A total 20 DNA-seq and 16 RNA-seq libraries were generated. After quality control and trimming, the DNA-seq libraries retained 13.9–20.9 million reads (96.3–98.2% of the original reads), corresponding to 1.9–2.8 Gb of sequence data (80.3–88.3% of the original data). The RNA-seq libraries retained 60.5–200.9 million reads (82.5–94.2%), corresponding to 6.9–21.4 Gb of sequence data (62.5–77.8%).

# ITS2-enriched Read Recovery and Assembly

Mapping against clade-specific *Symbiodiniaceae* ribosomal references recovered 0–40.2 × $10^3$ reads from the genome-skimming datasets, corresponding to 0–5,472 kb of sequence data. Assembly of these ITS2-enriched reads generated 1–365 contigs, with total assembly lengths ranging from 0.2 to 148.1 kb. In the transcriptomic datasets, 8–4,297 × $10^3$ reads were recovered after mapping against the *Symbiodiniaceae* reference sequences, corresponding to 1–559 kb of sequence data. The resulting assemblies comprised 13–17,412 contigs, with total assembly lengths ranging from 2 to 1,303 kb (Table 3).

Table 3

Summary of mapped reads, assemblies, and contigs recovered for each annotated ribosomal region (18S, ITS1, 5.8S, ITS2, and 28S) after mapping genome-skimming and transcriptomic reads of *Actinostella* spp. against genus-specific Symbiodiniaceae ribosomal references.

| *Approach* | Genus | Mapped | | Assembled | | Ribosomal region | | | | |
|---|---|---|---|---|---|---|---|---|---|---|
| | | **Total reads (×10³)** | **Total bases (kb)** | **No. of contigs** | **Total assembly length (kb)** | **18S** | **ITS1** | **5.8S** | **ITS2** | **28S** |
| Genome-skimming | *Breviolum* | 0.8–39.9 (5.4 ± 7.4) | 108–5,438 (725 ± 1,013) | 6–323 (24 ± 59) | 3.4–144.7 (10.7 ± 26.4) | 24 | 10 | 5 | 5 | 13 |
| | *Cladocopium* | 0–4.5 (0.7 ± 0.9) | 4–616 (88 ± 116) | 1–70 (5 ± 13) | 0.5–30.4 (2.3 ± 5.5) | 0 | 0 | 0 | 1 | 2 |
| | *Durusdinium* | 0–3.4 (0.4 ± 0.7) | 0–488 (60 ± 94) | 2–8 (3 ± 2) | 0.5–2.3 (1 ± 0.5) | 0 | 0 | 0 | 0 | 0 |
| | *Effrenium* | 0–3.6 (0.5 ± 0.7) | 0–488 (63 ± 99) | 1–8 (3 ± 2) | 0.2–2.5 (1.1 ± 0.5) | 0 | 0 | 0 | 0 | 0 |
| | *Freudenthalidium* | 0–3.2 (0.5 ± 0.6) | 0–435 (69 ± 86) | 2–10 (4 ± 2) | 0.5–2.4 (1.2 ± 0.5) | 0 | 0 | 0 | 0 | 0 |
| | *Fugacium* | 0–4.9 (0.6 ± 0.9) | 0–660 (85 ± 128) | 2–10 (4 ± 2) | 0.9–3.6 (1.4 ± 0.6) | 0 | 0 | 0 | 0 | 0 |
| | *Gerakladium* | 0–2.9 (0.4 ± 0.6) | 0–387 (52 ± 80) | 1–9 (3 ± 2) | 0.2–2.3 (1 ± 0.5) | 0 | 0 | 0 | 0 | 0 |
| | *Halluxium* | 0–4.6 (0.7 ± 0.9) | 0–621 (88 ± 121) | 3–12 (5 ± 2) | 0.9–2.8 (1.5 ± 0.5) | 0 | 0 | 0 | 0 | 0 |
| | *Symbiodinium* | 0.8–40.2 (5.3 ± 7.5) | 102–5,472 (711 ± 1,016) | 5–365 (27 ± 67) | 3.2–148.1 (11 ± 27) | 20 | 7 | 4 | 5 | 15 |
| Transcriptome | *Breviolum* | 177–4,335 (1,687 ± 1,381) | 21–559 (210 ± 174) | 117–17,412 (4,252 ± 5,021) | 15–1,303 (332 ± 377) | 26 | 13 | 0 | 1 | 4 |

| | | | | | | | | | |
|---|---|---|---|---|---|---|---|---|---|
| *Cladocopium* | 16–531 (197 ± 162) | 2–70 (26 ± 21) | 15–1,546 (365 ± 441) | 3–121 (30 ± 34) | 0 | 0 | 0 | 0 | 0 |
| *Durusdinium* | 9–195 (58 ± 44) | 1–22 (7 ± 5) | 17–629 (142 ± 175) | 3–50 (13 ± 13) | 0 | 0 | 0 | 0 | 0 |
| *Effrenium* | 9–189 (71 ± 57) | 1–21 (9 ± 7) | 17–770 (171 ± 191) | 3–63 (16 ± 15) | 0 | 0 | 0 | 0 | 0 |
| *Freudenthalidium* | 9–212 (88 ± 69) | 1–25 (11 ± 9) | 17–761 (226 ± 242) | 3–64 (20 ± 19) | 0 | 0 | 0 | 0 | 0 |
| *Fugacium* | 23–552 (116 ± 132) | 3–71 (14 ± 17) | 5–574 (143 ± 167) | 2–39 (12 ± 12) | 0 | 0 | 0 | 0 | 0 |
| *Gerakladium* | 8–187 (48 ± 42) | 1–21 (6 ± 5) | 13–394 (97 ± 96) | 3–31 (9 ± 7) | 0 | 0 | 0 | 0 | 0 |
| *Halluxium* | 26–570 (227 ± 173) | 3–74 (28 ± 21) | 17–754 (258 ± 196) | 3–59 (22 ± 15) | 0 | 0 | 0 | 0 | 0 |
| *Symbiodinium* | 177–4,297 (1,670 ± 1,364) | 21–550 (208 ± 173) | 123–16,385 (3,254 ± 4,710) | 16–1,232 (260 ± 357) | 47 | 17 | 22 | 16 | 53 |

Most annotated ribosomal contigs recovered from both genome-skimming and transcriptomic assemblies were assigned to *Symbiodinium* and *Breviolum* (Fig. 3 and Table 3). In the genome-skimming dataset, 18S and 28S (44 and 28 annotated contigs, respectively) were the most frequently recovered ribosomal regions, whereas ITS1, 5.8S, and ITS2 were represented by fewer annotated contigs (17, 9, and 10 annotated contigs, respectively; Table 3). Only a few annotated contigs were assigned to *Cladocopium*, restricted to the ITS2 and 28S regions (1 and 2 annotated contigs, respectively), whereas no annotated ribosomal contigs were recovered for the remaining Symbiodiniaceae genera. Transcriptomic assemblies showed consistently greater recovery across all ribosomal regions (72, 30, 22, 17, and 57 annotated contigs for the 18S, ITS1, 5.8S, ITS2, and 28S regions, respectively; Table 3).

Overall, ITS2 sequences were successfully recovered from 10 of the 20 genome-skimming samples (50%) and from all 16 transcriptomic samples (100%). Multiple distinct ITS2 sequence variants were detected in two individuals. FLK-01 yielded three distinct ITS2 sequence variants, two assigned to *Symbiodinium* and one to *Breviolum*, whereas CI-SP-1 yielded two distinct *Breviolum* ITS2 sequence variants. The genome-skimming dataset recovered ITS2 sequences assigned to *Symbiodinium* (N = 5), *Breviolum* (N = 5), and *Cladocopium* (N = 1), whereas transcriptomic data recovered predominantly *Symbiodinium* ITS2 sequences (N = 17), with *Breviolum* detected in a single sample. Where sequence identity permitted, recovered ITS2 sequences matched previously described SymPortal ITS2 profiles, including A4, A4f, B1, and 71568_A, whereas several sequences could only be assigned confidently to Symbiodiniaceae genera because they did not correspond unambiguously to an existing reference profile (Fig. 4 and Supplementary Tables S1–S3).

# ITS2 Phylogenetic Relationships

The maximum-likelihood phylogeny revealed geographically widespread associations between *Actinostella* populations and three genera of Symbiodiniaceae (Fig. 4 and Supplementary Table S4). *Symbiodinium* sequences were recovered from *Actinostella* populations across the western Atlantic, including the Florida Keys, USA (FLK and NSK), Yucatán, Mexico (YU_Me), and northeastern Brazil (MA_Br and SBA). These sequences clustered into a strongly supported lineage (SH-aLRT/UFBoot = 98.7/99%). *Breviolum* was represented by sequences recovered from *Actinostella* populations from the Canary Islands (CI_SP), Florida Keys (FLK), Florianópolis (FSC), Salvador, Bahia (SBA), and Ubatuba, São Paulo (UB_Br and USP), forming a strongly supported lineage (SH-aLRT/UFBoot = 99.6/100%). *Cladocopium* was represented by fewer sequences, including samples from Cabo Frio, Rio de Janeiro (CFRJ), Salvador, Bahia (SBA), and Ubatuba, São Paulo (USP), which clustered together with moderate to strong support (SH-aLRT/UFBoot = 93.3/87%). The recovered Symbiodiniaceae lineages included sequences from multiple *Actinostella* populations and geographic regions, without clustering exclusively by sampling locality.

# DISCUSSION

By integrating targeted ITS2 metabarcoding with Symbiodiniaceae sequences recovered from transcriptomic and genome-skimming datasets, this study provides the first broad-scale assessment of symbiont diversity associated with *Actinostella* spp. across multiple regions of the Atlantic Ocean. The application of the SymPortal analytical framework (Hume et al. 2019) enabled high-resolution characterisation of ITS2 diversity in Brazilian populations, while the complementary sequencing datasets expanded the geographic and taxonomic scope of our analyses by including additional locations of *A. flosculifera*, *A. yucatanensis*, and *Actinostella* sp. Together, these approaches revealed a diverse Symbiodiniaceae assemblage composed primarily of *Breviolum*, *Symbiodinium*, and *Cladocopium*, with variation in their occurrence among host species, geographic regions, and individual specimens. Across the three *Actinostella* taxa examined, *Breviolum* was recovered from all hosts, whereas *Symbiodinium* was detected only in *A. flosculifera* and *A. yucatanensis*, and *Cladocopium* only in *A. flosculifera*.

Our results indicate that Symbiodiniaceae communities associated with *Actinostella* are structured by biogeographic and local-scale processes, consistent with the emerging view that benthic cnidarian holobionts respond simultaneously to regional and local environmental gradients (Clerissi et al. 2026; Davies et al. 2023; Parkinson et al. 2025; Ruggeri et al. 2024). *Breviolum* is common to all species of *Actinostella*, but specific strains vary across hosts and localities. *Symbiodinium* and *Cladocopium* were more narrowly distributed in the samples examined, with *Symbiodinium* detected in samples of both *A. flosculifera* and *A. yucatanensis*, whereas *Cladocopium* was detected only in *A. flosculifera*. This pattern indicates that the occurrence of these symbiont genera varied among host species and geographic regions within the sampling of this study.

**Breviolum is the core symbiont of Actinostella spp.**

Across all methods for assaying symbiont identity, *Breviolum* emerged as a major component of the Symbiodiniaceae community associated with *Actinostella* spp. In the metabarcoding dataset, *Breviolum* was detected in all metabarcoded specimens and represented 38.2–100% of post-MED reads, with five ITS2 profiles (B1, B14a, B1au, B1g, and 29445_B) shared between the tropical and subtropical Brazilian populations. The broader dataset provided additional context for this pattern. ITS2 sequences assigned to *Breviolum* were also recovered from the genome-skimming and transcriptomic datasets and included previously described ITS2 profiles (e.g., B1; Supplementary Table S2), as well as additional *Breviolum* lineages recovered from geographically distant *Actinostella* populations in both the Western and Eastern Atlantic. Thus, although *Breviolum* was not detected in every individual across the broader dataset, its occurrence across multiple host species, geographic regions, and sequencing approaches indicates that associations with *Breviolum* are geographically widespread within *Actinostella*. The widespread presence of *Breviolum* across hosts and regions suggests

it is a stable component of the symbiotic repertoire in the sampled *Actinostella* species. However, the limited sample size of the metabarcoded samples and low sequencing depth of the genome-skimming and transcriptomic datasets preclude its designation as a universal or core symbiont of the genus.

The widespread occurrence of *Breviolum* across the *Actinostella* taxa examined suggests that members of this *Breviollum* may represent recurrent symbiotic partners in the genus *Actinostella*. However, the ecological significance of this association remains uncertain because symbiont identity can influence host physiological performance under environmental stress (Lust et al. 2025). Because our ITS2 data do not resolve species-level identities or directly assess symbiont function, the recurrent detection of *Breviolum* should be interpreted as evidence of a widespread association rather than an adaptive advantage.

At a finer geographic scale, the metabarcoding dataset also revealed differences in Symbiodiniaceae community composition between the Brazilian populations. UPGMA clustering based on Bray–Curtis dissimilarity separated specimens from SBA and USP without incorporating geographic information (Fig. 2). Between-region dissimilarity (mean = 0.702) was higher than within-region dissimilarity (mean SBA = 0.667; mean USP = 0.476), while the two most similar specimens, USP-1 and USP-9 (BC = 0.026), originated from the same region. Although the small and uneven sample size precludes inferences about the mechanisms underlying this pattern, these results suggest geographic structuring of Symbiodiniaceae community composition at the regional scale. Such differentiation may reflect local environmental conditions, regional symbiont availability, or other ecological factors, but additional standardized sampling and environmental data are required to distinguish among these alternatives.

**Symbiodinium as a tropical accessory layer**

The targeted metabarcoding dataset revealed a clear regional pattern in the distribution of *Symbiodinium* among the Brazilian populations examined. All eight *Symbiodinium* ITS2 profiles recovered by metabarcoding were detected in tropical SBA, whereas *Symbiodinium* was not detected in the four specimens from subtropical USP. In Salvador, however, *Symbiodinium* accounted for only 24–39% of reads, occurring alongside the predominant *Breviolum* component. This regional pattern is consistent with the broader geographic dataset, in which ITS2 sequences assigned to *Symbiodinium* were also recovered from samples from Pernambuco, Yucatán, and the Florida Keys and were recovered from both *A. flosculifera* and *A. yucatanensis*. These sequences comprised multiple ITS2 lineages (Supplementary Table S3), including the A4 profile, A4f, 71568_A, and additional *Symbiodinium* sequences that could not be assigned confidently to a previously described SymPortal profile, indicating that the observed geographic distribution reflects several *Symbiodinium* lineages rather than a single widespread lineage. These findings show that associations with *Symbiodinium* occur in geographically distant *Actinostella* populations across the Western Atlantic. The present sampling did not allow environmental or latitudinal factors to be identified as drivers of this distribution or to assess whether and how, for example, relative abundance shifts across geography. Differences in sampling effort, tissue source, and sequencing methodology among localities preclude direct comparisons of prevalence or relative abundance across the entire geographic range. Further standardized sampling will be necessary to determine whether the distribution of *Symbiodinium* is associated with latitude, local environmental conditions, host identity, or other ecological factors.

**Heterogeneous occurrence of Cladocopium across Actinostella populations**

The metabarcoding dataset revealed a heterogeneous distribution of *Cladocopium* among individual *Actinostella flosculifera* hosts. Although *Cladocopium* was not consistently present, it represented more than 35% of reads in one individual from each sampled region: SBA-2, which harboured C1, C1b, and five additional DIVs, and USP-10, in which C3 was detected. The specific composition of *Cladocopium* also differed between these individuals, indicating variation in assemblages detected in the tropical and subtropical populations. However, because high *Cladocopium* abundance was

restricted to a few individual specimens and environmental variables were not measured, the factors underlying this variation remain unresolved.

The broader dataset provides additional evidence for associations between *Actinostella* and *Cladocopium*. *Cladocopium* ITS2 sequences were also recovered from *A. flosculifera* samples from CFRJ, SBA, and USP using the complementary sequencing datasets. Together, these observations indicate that *Cladocopium* occurs in geographically separated populations of *A. flosculifera*, although their detection and apparent prevalence varied among samples and sequencing approaches.

The occurrence of *Cladocopium* at relatively high abundances in some individuals raises the possibility that less consistently represented symbiont lineages may contribute to variation in the symbiotic repertoire of *Actinostella*. Changes in the relative abundance of symbiont lineages already present within a host community have been discussed as a potential component of holobiont responses to environmental change (Cavailles et al. 2025; MacVittie et al. 2024). Nevertheless, the present study does not allow us to determine whether the observed variation in *Cladocopium* abundance reflects temporal changes, environmental selection, microhabitat conditions, or stable differences among individual hosts. Longitudinal and experimental studies will therefore be required to determine whether *Cladocopium* contributes to variation in the symbiotic community of *Actinostella* under changing environmental conditions.

## Within-region heterogeneity in Symbiodiniaceae community composition

The fine-scale variation observed within our targeted metabarcoding dataset revealed substantial differences among conspecific *Actinostella flosculifera* individuals at the sub-generic level. Within Ubatuba, for instance, the four individuals examined in this study, whose taxonomic identity was confirmed through morphological and molecular analyses (Durán-Fuentes et al. 2026), shared a common dominance of *Breviolum*, but differed markedly in the composition and relative abundance of their ITS2 profiles. B1au was the dominant profile in USP-5 (65.6%), whereas 29445_B dominated USP-1 (34.0%) and B14a represented the most abundant profile in USP-9 (25.9%). In contrast, *Cladocopium* C3 was detected exclusively in USP-10, where it accounted for 35.7% of the recovered ITS2 profiles (Fig. 2 and Table 2). This variation among conspecific *Actinostella flosculifera* individuals from the same locality resembles the microhabitat-driven sub-generic turnover described by Ruggeri et al. (2024) in the intertidal sea anemone *Anthopleura elegantissima* (Brandt, 1835) at Shark Harbor, Catalina Island, California, USA, where differences between high and low intertidal zones and microhabitat positions within aggregations were associated with shifts in ITS2 variant composition within dominant Symbiodiniaceae lineages.

The three specimens from SBA-showed a different pattern, consistently combining a *Symbiodinium* component with a *Breviolum* backbone, while differing in the contribution of less dominant lineages. *Breviolum* was detected only in sample SBA-2, where C1 was the dominant profile (20.1%) together with additional C-type profiles, whereas SBA-1 and SBA-3 lacked detectable *Cladocopium* (Fig. 2 and Table 2). Furthermore, variation in *Symbiodinium* diversity was observed among individuals, with SBA-3 exhibiting the highest richness (eight ITS2 profiles). Together, the within-region heterogeneity observed at both sites suggests that variation among *Actinostella* individuals was expressed primarily through differences in the relative contribution of Symbiodiniaceae lineages and DIVs within a shared genus-level framework, rather than shifting through complete replacement of the dominant symbiotic community.

## Complementary insights from genome-skimming and transcriptome datasets

Symbiodiniaceae ITS2 sequences provide valuable complementary insights for holobiont studies. Similar approaches have recently been applied in scleractinian corals, where host-focused genome-skimming datasets were leveraged to

characterize Symbiodiniaceae associations by capturing symbiont-derived reads and ITS2 profiles (Connelly et al. 2026). Here, we expanded this concept by applying a mapping-based ITS2 extraction workflow to both genome-skimming and transcriptomic datasets, enabling the retrieval of Symbiodiniaceae ribosomal markers without targeted symbiont sequencing.

The complementary genome-skimming and transcriptomic datasets expanded the geographic and taxonomic scope of the targeted metabarcoding dataset while providing a different perspective on Symbiodiniaceae diversity. Transcriptomic datasets showed particularly high recovery success, with ITS2 sequences detected in all analyzed samples (100%). This high recovery was expected because these transcriptomic libraries were generated from the marginal ruff, a tissue region directly exposed to light and enriched in Symbiodiniaceae cells and ribosomal transcripts. These datasets recovered predominantly *Symbiodinium* ITS2 sequences, with *Breviolum* detected in a single sample. In contrast, genome-skimming recovered ITS2 sequences in only 10 out of 20 analysed specimens (50%). Although lower, this recovery rate was also expected because these libraries were originally generated from pedal disc tissue for independent genomic analyses, a region generally located in shaded portions of the organism and selected because it was expected to contain lower densities of photosymbionts. Nevertheless, genome-skimming recovered representatives of all three Symbiodiniaceae genera detected in this study (*Symbiodinium*, *Breviolum*, and *Cladocopium*), extending their detection across geographically separated *Actinostella* populations.

Although these complementary datasets cannot be directly compared quantitatively with SymPortal-resolved metabarcoding because of differences in tissue source, sequencing strategy, sequencing depth, and detection sensitivity, they independently corroborated the occurrence of the three major Symbiodiniaceae genera identified by targeted metabarcoding. In contrast, the fine-scale ITS2 diversity resolved by SymPortal would likely remain undetected using broader genome-scale sequencing approaches, highlighting the importance of dedicated ITS2 metabarcoding for resolving intra-population variability in non-coral cnidarian symbioses (Hume et al. 2019).

Even so, we generally recovered fewer Symbiodiniaceae ITS2 variants using these “by catch” approaches than by direct ITS2 metabarcoding. Targeted metabarcoding recovered an average of 8.7 ITS2 profiles per *Actinostella* specimen, whereas the transcriptomic dataset generally recovered a single predominant ITS2 sequence per sample and the genome-skimming dataset recovered one to three ITS2 sequences per successful sample. These differences likely reflect both biological and methodological factors. Besides differences among the samples analysed, genome-skimming and transcriptomic datasets recover Symbiodiniaceae sequences only incidentally, and rare ITS2 variants are therefore less likely to be retained following normalization, assembly, and quality-filtering procedures than in dedicated ITS2 metabarcoding analyses. Consequently, although these “by catch” approaches cannot replace targeted ITS2 metabarcoding for high-resolution characterization of Symbiodiniaceae communities, they substantially increase the biological value that can be extracted from existing sequencing datasets while avoiding additional sampling and library preparation.

## Limitations and future directions

Several limitations of this study should be noted, particularly regarding the sample distribution of the 43 specimens analyzed. Because biological replicates were unevenly distributed across host species, localities, and sequencing platforms, comprising targeted ITS2 metabarcoding (N = 7), genome-skimming (N = 20), and transcriptomics (N = 16), formal geographic comparisons of Symbiodiniaceae communities were constrained. Consequently, our findings offer an exploratory snapshot of Symbiodiniaceae diversity and distribution within the anemone genus *Actinostella* across the Atlantic, rather than a balanced quantitative comparison among populations or species.

The integration of ITS2 metabarcoding, genome-skimming, and transcriptomic datasets provides complementary information but also introduces important methodological and tissue-specific differences. ITS2 metabarcoding was

specifically designed to characterise Symbiodiniaceae diversity at high resolution. In contrast, the genome-skimming data were originally generated for a different research objective using DNA extracted from pedal disc tissue, whereas the transcriptomic datasets analysed here were derived from marginal ruff tissue, a structure conspicuously enriched in Symbiodiniaceae and targeted in the ITS2 metabarcoding data collection. These differences in tissue origin, sequencing strategy, sequencing depth, and detection sensitivity likely contributed to the contrasting recovery of ITS2 sequences among datasets, particularly the lower recovery observed in the genome-skimming samples compared with the transcriptomic dataset. Differences in Symbiodiniaceae composition and relative abundance associated with light-exposed versus shaded regions have also been documented within individual cnidarian hosts (Lewis et al. 2022), supporting the possibility that tissue-specific sampling may contribute to differences in symbiont detection. For the metabarcoding dataset, taxonomic assignment was based on the SymPortal-curated reference database, and therefore highly divergent or poorly represented Symbiodiniaceae lineages may not have been assigned. For the genome-skimming and transcriptomic datasets, we additionally performed an independent mapping approach using representative ITS2 sequences from different Symbiodiniaceae genera, which recovered sequences corresponding to *Symbiodinium*, *Breviolum*, and *Cladocopium*.

Therefore, failure to recover a Symbiodiniaceae lineage from a genome-skimming sample should not be interpreted as evidence of its biological absence, and direct quantitative comparisons of symbiont abundance among the three sequencing approaches should be avoided. Nevertheless, the genome-skimming and transcriptomic datasets provide independent evidence for the occurrence of *Symbiodinium*, *Breviolum*, and *Cladocopium* beyond the Brazilian metabarcoding dataset by extending taxonomic coverage to *A. yucatanensis* and *Actinostella* sp. and geographic coverage to additional populations across the Western and Eastern Atlantic.

Third, the cross-sectional sampling design provides a spatial snapshot of Symbiodiniaceae diversity and does not capture temporal, seasonal, or post-disturbance changes in symbiont composition. Therefore, the present data cannot directly evaluate dynamic processes such as symbiont shuffling or switching. Longitudinal sampling before, during, and after marine heatwaves would be necessary to determine whether the broad symbiont repertoire documented here contributes to the capacity of *Actinostella* spp. to reorganise their symbiotic associations under environmental stress (Bennett-Smith et al. 2025; Buzzoni et al. 2026).

Finally, the present study does not directly link Symbiodiniaceae identity or community composition to host physiological state or local environmental variables, such as temperature, irradiance, and salinity. Future studies should combine standardised SymPortal-resolved profiling across a broader and more balanced geographic sampling design with environmental monitoring and holobiont physiological assays, as applied to intertidal anemone systems by Ruggeri et al. (2024). Applying targeted and standardised Symbiodiniaceae profiling to the same tissue type across *Actinostella* species and populations would also allow more robust comparisons of host specificity and biogeographic structure. Such an integrated approach would help disentangle the relative contributions of host identity, geography, environmental filtering, tissue-specific symbiont distribution, and methodological detection to the patterns observed in *Actinostella* spp.

## CONCLUSIONS

The integration of ITS2 metabarcoding through the SymPortal analytical framework with complementary genome-skimming and transcriptomic datasets provided the first high-resolution assessment of Symbiodiniaceae diversity associated with *Actinostella* spp. across Atlantic populations. Broadly, we find variation in the Symbiodinaceae community within and among populations and species of *Actinostella*. This includes variation in the major lineage (genera) of the symbionts present, the specific identities of the constituents within each symbiont lineage, and in the prevalence of each major lineage. Variation has some elements that are geographically structured, and some elements that are not; likewise there are hints of some difference between species of host, although those are not fully developed because of limitations in sampling. Three  specific conclusions emerge from this work: 1) *Breviolum* lineages represent a

widespread and recurrent component of *Actinostella* associations on the Brazilian coast, detected in all metabarcoded specimens and characterised by a shared set of ITS2 profiles (B1, B14a, B1au, B1g, and 29445_B) connecting tropical Northeast and subtropical Southeast populations. Complementary genome-skimming and transcriptomic datasets further supported the broad occurrence of *Breviolum* across multiple *Actinostella* populations and host groups. 2) The Symbiodiniaceae community associated with *Actinostella* is composed of multiple genera, including *Breviolum*, *Symbiodinium*, and *Cladocopium*, with their relative contributions varying among regions and individuals. High-resolution metabarcoding revealed regional and within-population variation in ITS2 profiles, whereas genome-skimming and transcriptomic data expanded the detection of these major symbiont lineages across the Atlantic distribution of the genus. 3) The occurrence of multiple Symbiodiniaceae lineages across *Actinostella* spp. indicates a diverse symbiotic repertoire that may contribute to ecological flexibility across tropical and subtropical environments. Although future experimental studies are required to directly evaluate mechanisms such as symbiont shuffling and switching, this work establishes *Actinostella* as a promising model for investigating Symbiodiniaceae diversity and host–symbiont dynamics in non-coral cnidarians under environmental change.

## Declarations

# ACKNOWLEDGEMENTS

This work was supported by the Coordenação de Aperfeiçoamento de Pessoal de Nível Superior — CAPES (No. 88887.952891/2024-00) and by the Fundação de Amparo à Pesquisa do Estado de São Paulo — FAPESP 2021/06274-1, 2021/10639-5, 2022/16193-1, 2022/09430-7, 2023/10683-0, and 2024/23482-5). SNS was supported by CNPq (Research Productivity Scholarship) grant number 304267/2022-8 and 302100/2026-1. We thank the SymPortal team for maintaining the curated reference database and analytical framework used in this study. EL lab is supported by CNPq (406993/2023-8, INC0006/2019, 408930/2024-1, 404514/2025-1).

# DATA AVAILABILITY

Raw paired-end sequencing reads, the SymPortal sample-metadata table, post-MED count table, and the seven *Actinostella flosculifera* ITS2 type-profile assignments are available under the SymPortal dataset 20260327T192550_stampse1 (DSU 1460; sample UIDs 267840–267846). Voucher photographs and associated field metadata are archived at the Coleção Zoológica da Faculdade de Ciências de Bauru, UNESP.

The transcriptomic data are available under NCBI BioProject accession PRJNA1430975, with BioSample accessions SAMN56295681–SAMN56295709 and Sequence Read Archive (SRA) accessions SRR37440179–SRR37440207. The genome-skimming data are available under BioProject accession PRJNA1191889, with BioSample accessions SAMN45095338–SAMN45095359 and SRA accessions SRR31545956–SRR31545981.

ITS2 sequences generated from metabarcoding, transcriptomic, and genome-skimming datasets have been deposited in NCBI GenBank under accession numbers PZ622654–PZ622715, PZ626986–PZ627003, and PZ629999–PZ630009, respectively.

## AUTHOR CONTRIBUTIONS

JDF and SNS conceptualized the study, performed formal analyses, curated the data, developed the methodology, created visualizations, and wrote the original manuscript draft. AMR, JDF, MD, JMM, EL, TBS and SNS contributed to the research design and sampling specimens. AMR, MD, TBS and SNS contributed to funding acquisition and project administration. All authors reviewed and edited the manuscript and approved the final version.

**FUNDING DECLARATION**

This work was supported by the Coordenação de Aperfeiçoamento de Pessoal de Nível Superior — CAPES (No. 88887.952891/2024-00) and by the Fundação de Amparo à Pesquisa do Estado de São Paulo — FAPESP 2021/06274-1, 2021/10639-5, 2022/16193-1, 2022/09430-7, 2023/10683-0, and 2024/23482-5). SNS was supported by CNPq (Research Productivity Scholarship) grant number 304267/2022-8 and 302100/2026-1. EL lab is supported by CNPq (406993/2023-8, INC0006/2019, 408930/2024-1, 404514/2025-1).

# References

1. Anthony CJ, Lemer S, Raymundo LJ, Rouzé H (2025) Restoration innovation: Fusing microbial memories to engineer coral resilience. *One Earth* 8(2). https://doi.org/10.1016/j.oneear.2025.101193
2. Baker AC (2003) Flexibility and specificity in coral-algal symbiosis: diversity, ecology, and biogeography of *Symbiodinium*. Annu Rev Ecol Evol Syst 34(1), 661–689. https://doi.org/10.1146/annurev.ecolsys.34.011802.132417
3. Bankevich A, Nurk S, Antipov D, Gurevich AA, Dvorkin M, Kulikov AS, Lesin VM, Nikolenko SI, Pham S, Prjibelski AD, Pyshkin AV, Sirotkin AV, Vyahhi N, Tesler G, Alekseyev MA, Pevzner PA (2012) SPAdes: a new genome assembly algorithm and its applications to single-cell sequencing. J Comput Biol 19(5), 455–477. https://doi.org/10.1089/cmb.2012.0021
4. Barragán Y, Rodríguez E, Chiodo T, Gusmão LC, Sánchez C, Lauretta D (2024) Revision of the genus *Actinostella* (Cnidaria: Actiniaria: Actinioidea) from tropical and subtropical western Atlantic and eastern Pacific: redescriptions and synonyms. Am Mus Novit 1–48. https://doi.org/10.1206/4014.1
5. Beauson E (2025) Temperate Symbiodiniaceae physiology and behavior in the context of the cnidarian–dinoflagellate symbiosis. Doctoral dissertation, Université Côte d'Azur. https://theses.hal.science/tel-05565401/
6. Bell SL, Quigley KM (2025) Global free-living Symbiodiniaceae biodiversity mirrors local environments. J Biogeogr 52(7), e15137. https://doi.org/10.1111/jbi.15137
7. Bennett-Smith MF, Villela H, Justo MSS, Carvalho S, Voolstra CR, Berumen ML (2025) Near complete local extinction of iconic anemonefish and their anemone hosts following a heat stress event. *npj Biodiversity* 4, 107. https://doi.org/10.1038/s44185-025-00107-4
8. Botana MT (2025) Lipid mediators and a new HOPE in the cnidarian–dinoflagellate symbiosis. Doctoral dissertation, Te Herenga Waka — Victoria University of Wellington. https://openaccess.wgtn.ac.nz/articles/thesis/29338721
9. Buddemeier RW, Fautin DG (1993) Coral bleaching as an adaptive mechanism. Bioscience 43(5), 320–326. https://doi.org/10.2307/1312064
10. Buzzoni D, Van Nynatten A, Cunning R, Baker AC, McManus LC (2026) Persistent legacy effects of marine heatwaves on coral symbioses. Glob Change Biol 32, e70818. https://doi.org/10.1111/gcb.70818
11. Camacho C, Coulouris G, Avagyan V, Ma N, Papadopoulos J, Bealer K, Madden TL (2009) BLAST+: architecture and applications. BMC Bioinformatics 10, 421. https://doi.org/10.1186/1471-2105-10-421
12. Cavailles J, Kuzmics C, Grube M (2025) Symbiont dynamics and coral regulation under changing temperatures. Coral Reefs 44, 1–14. https://doi.org/10.1007/s00338-025-02667-0
13. Chen S (2025) fastp 1.0: An ultra-fast all-round tool for FASTQ data quality control and preprocessing. Imeta, 4(5), e70078. https://doi.org/10.1002/imt2.70078
14. Clerissi C, Beldade R, Mejaït A, Haguenauer A, Jobet E, Mills SC (2026) Microbiota of host sea anemones and their associated anemonefish show contrasting responses to a bleaching event. Coral Reefs 45, 817–830. https://doi.org/10.1007/s00338-025-02799-3
15. Coleman AW, Suarez A, Goff LJ (1994) Molecular delineation of species and syngens in volvocacean green algae (Chlorophyta). J Phycol 30(1), 80–90. https://doi.org/10.1111/j.0022-3646.1994.00080.x

16. Connelly MT, Glynn VM, Cornejo A, Villalobos-Cubero T, Kleypas J, Alvarado JJ, Brandt M, Logan CA, Palacio-Castro AM, Flot JF, Leray M, Connolly SR, Quattrini AM (2026) Genome skimming illuminates hidden species diversity and Symbiodiniaceae associations in east Pacific *Pocillopora* corals. Genome Biol Evol 18(2), evaf235. https://doi.org/10.1093/gbe/evaf235
17. Crehan O (2025) The role of nitrogen metabolism in the stability and dysfunction of the cnidarian–dinoflagellate symbiosis. Doctoral dissertation, Te Herenga Waka — Victoria University of Wellington. https://openaccess.wgtn.ac.nz/articles/thesis/30105154
18. Danecek P, Bonfield JK, Liddle J, Marshall J, Ohan V, Pollard MO, Li H (2021) Twelve years of SAMtools and BCFtools. Gigascience 10(2), giab008. https://doi.org/10.1093/gigascience/giab008
19. Daly M, Chaudhuri A, Gusmão L, Rodríguez E (2008) Phylogenetic relationships among sea anemones (Cnidaria: Anthozoa: Actiniaria). Mol Phylogenet Evol 48(1), 292–301. https://doi.org/10.1016/j.ympev.2008.02.022
20. Davies SW, Gamache MH, Howe-Kerr LI, Kriefall NG, Baker AC, Banaszak AT, Bay LK, Bellantuono AJ, Bhattacharya D, Chan CX, Claar DC, Coffroth MA, Cunning R, Davy SK, del Campo J, Díaz-Almeyda EM, Frommlet JC, Fuess LE, González-Pech RA, Goulet TL, Hoadley KD, Howells EJ, Hume BCC, Kemp DW, Kenkel CD, Kitchen SA, LaJeunesse TC, Lin S, McIlroy SE, McMinds R, Nitschke MR, Oakley CA, Peixoto RS, Prada C, Putnam HM, Quigley K, Reich HG, Reimer JD, Rodriguez-Lanetty M, Rosales SM, Saad OS, Sampayo EM, Santos SR, Shoguchi E, Smith EG, Stat M, Stephens TG, Strader ME, Suggett DJ, Swain TD, Tran C, Traylor-Knowles N, Voolstra CR, Warner ME, Weis VM, Wright RM, Xiang T, Yamashita H, Ziegler M, Correa AMS, Parkinson JE (2023) Building consensus around the assessment and interpretation of Symbiodiniaceae diversity. PeerJ 11, e15023. https://doi.org/10.7717/peerj.15023
21. DeBiasse M, Buckenmeyer A, Macrander J, Babonis L, Bentlage B, Cartwright P, Prada C, Reitzel A, Stampar S, Collins A, Daly M, Ryan J (2024) A cnidarian phylogenomic tree fitted with hundreds of 18S leaves. Bull Soc Syst Biol 3(2). https://doi.org/10.18061/bssb.v3i2.9267
22. del Campo J, Bonacolta AM, Weiler BA, Knowles B, 'Ohana Marine Microbiome Consortium. (2026) Global diversity and distribution of coral-associated protists. bioRxiv. https://doi.org/10.1101/2026.01.22.700988
23. Durán-Fuentes JA, Gracia A, González-Muñoz R (2022) Sea anemones (Cnidaria, Anthozoa, Actiniaria) in high sedimentation environments influenced by the Magdalena River (Colombian Caribbean). An Acad Bras Ciênc 94, e20190862. https://doi.org/10.1590/0001-3765202120190862
24. Duran-Fuentes JA, Mendes F, Da Costa RC, Pescinelli RA, Floeter SR, Stampar SN (2023) Ecological notes on *Actinostella flosculifera* (Le Sueur, 1817) (Cnidaria: Actiniaria: Actiniidae) in the Southwestern Atlantic, Brazil. J. Mar Biol Assoc U.K. 103, e20. https://doi.org/10.1017/S0025315423000103
25. Durán-Fuentes JA, González-Muñoz R, Lizaola-Guillermo JM, Mendes F, Brandão R, Gomes PB, Pereira S, Santana ACP, Stampar NS (2026) Advancing our knowledge of *Actinostella*: a new species from Yucatan, Mexico, and comprehensive redescription of *A. flosculifera* (Le Sueur, 1817) (Cnidaria, Actiniaria). Mar Biodiv, 56, 78. https://doi.org/10.1007/s12526-026-01687-5
26. Emelianenko V, Santos MEA, Kim G, Husnik F (2026) Comparing Symbiodiniaceae diversity across unicellular hosts, multicellular hosts, and environmental reservoirs. bioRxiv. https://doi.org/10.1101/2026.04.21.719777
27. Eren AM, Morrison HG, Lescault PJ, Reveillaud J, Vineis JH, Sogin ML (2015) Minimum entropy decomposition: Unsupervised oligotyping for sensitive partitioning of high-throughput marker gene sequences. *The ISME Journal* 9(4), 968–979. https://doi.org/10.1038/ismej.2014.195
28. Fautin DG, Malarky L, Soberon J (2013) Latitudinal diversity of sea anemones (Cnidaria: Actiniaria). Biol Bull 224(2), 89–98. https://doi.org/10.1086/BBLv224n2p89
29. Fensome RA, Taylor FJR, Norris G, Sarjeant WAS, Wharton DI, Williams GL (1993) A classification of living and fossil dinoflagellates. Micropaleontology Spec Publ 7, 351.

30. Gamache MH (2025) Improving coral restoration outcomes through novel molecular applications. Doctoral dissertation, University of South Florida. USF ScholarCommons. https://digitalcommons.usf.edu/etd/12383
31. Glass BH (2025) Sensitivity and resilience of cnidarian early life processes to anthropogenic climate change. Doctoral dissertation, University of Pennsylvania. UPenn ScholarlyCommons. https://repository.upenn.edu/
32. González-Muñoz R, Simoes N, Sanchez-Rodriguez J, Rodríguez E, Segura-Puertas L (2012) First inventory of sea anemones (Cnidaria: Actiniaria) of the Mexican Caribbean. Zootaxa 3556, 1–38. https://doi.org/10.11646/zootaxa.3556.1.1
33. González-Muñoz R, Simões N, Tello-Musi JL, Rodríguez E (2013) Sea anemones (Cnidaria, Anthozoa, Actiniaria) from coral reefs in the southern Gulf of Mexico. ZooKeys 341, 77–106. https://doi.org/10.3897/zookeys.341.5816
34. Grabherr MG, Haas BJ, Yassour M, Levin JZ, Thompson DA, Amit I, Adiconis X, Fan L, Raychowdhury R, Zeng Q, Chen Z (2011) Full-length transcriptome assembly from RNA-Seq data without a reference genome. Nat Biotechnol 29, 644–652. https://doi.org/10.1038/nbt.1883
35. Guiry MD, Guiry GM (2026) AlgaeBase. World-wide electronic publication, National University of Ireland, Galway (taxonomic information republished from AlgaeBase with permission of M.D. Guiry). Symbiodiniaceae Fensome, Taylor, Norris, Sarjeant, Wharton & Williams, 1993. Accessed through: World Register of Marine Species at: https://www.marinespecies.org/aphia.php?p=taxdetails&id=109445 on 2026-07-06
36. Herrera-Bojórquez LG, González-Muñoz R, León-Deniz LV, Sima-Álvarez R (2020) Sea anemones (Anthozoa: Actiniaria) from the coast of Yucatán, Mexico. Rev Mex Biodivers 91, e913195. https://doi.org/10.22201/ib.20078706e.2020.91.3195
37. Hoang DT, Chernomor O, Von Haeseler A, Minh BQ, Vinh LS (2018) UFBoot2: improving the ultrafast bootstrap approximation. Mol Biol Evol 35(2), 518–522. https://doi.org/10.1093/molbev/msx281
38. Hume BCC, Smith EG, Ziegler M, Warrington HJM, Burt JA, LaJeunesse TC, Wiedenmann J, Voolstra CR (2019) SymPortal: A novel analytical framework and platform for coral algal symbiont next-generation sequencing ITS2 profiling. Mol Ecol Res 19(4), 1063–1080. https://doi.org/10.1111/1755-0998.13004
39. Kalyaanamoorthy S, Minh BQ, Wong TK, Von Haeseler A, Jermiin LS (2017) ModelFinder: fast model selection for accurate phylogenetic estimates. Nat Methods 14(6), 587–589. https://doi.org/10.1038/nmeth.4285
40. Katoh K, Standley DM (2013) MAFFT multiple sequence alignment software version 7: improvements in performance and usability. Mol Biol Evol 30(4), 772–780. https://doi.org/10.1093/molbev/mst010
41. LaJeunesse TC, Trench RK (2000) Biogeography of two species of *Symbiodinium* (Freudenthal) inhabiting the intertidal sea anemone *Anthopleura elegantissima* (Brandt). Biol Bull 199(2), 126–134. https://doi.org/10.2307/1542872
42. LaJeunesse TC (2002) Diversity and community structure of symbiotic dinoflagellates from Caribbean coral reefs. Mar Biol 141(2), 387–400. https://doi.org/10.1007/s00227-002-0829-2
43. LaJeunesse TC (2017) Validation and description of *Symbiodinium microadriaticum*, the type species of *Symbiodinium* (Dinophyta). J Phycology 53(5), 1109–1114. https://doi.org/10.1111/jpy.12570
44. LaJeunesse TC, Parkinson JE, Gabrielson PW, Jeong HJ, Reimer JD, Voolstra CR, Santos SR (2018) Systematic revision of Symbiodiniaceae highlights the antiquity and diversity of coral endosymbionts. Current Biol 28(16), 2570–2580. https://doi.org/10.1016/j.cub.2018.07.008
45. Lewis RE, Davy SK, Gardner SG, Rongo T, Suggett DJ, Nitschke MR (2022) Colony self-shading facilitates Symbiodiniaceae cohabitation in a South Pacific coral community. Coral Reefs 41(5), 1433–1447. https://doi.org/10.1007/s00338-022-02292-1
46. Li H, Durbin R (2009) Fast and accurate short read alignment with Burrows-Wheeler transform, Bioinformatics 25(14), 1754–1760, https://doi.org/10.1093/bioinformatics/btp324

47. Lust B, Matthews JL, Oakley CA, Grossman AR, Davy SK, Tortorelli G (2025) The influence of symbiont identity on the proteomic and metabolomic responses of the model cnidarian *Aiptasia* to thermal stress. *Environ Microbiol* 27, e70073. https://doi.org/10.1111/1462-2920.70073
48. Nitschke MR, Craveiro SC, Brandão C, Fidalgo C, Serôdio J, Calado AJ, Frommlet JC (2020) Description of *Freudenthalidium* gen. nov. and *Halluxium* gen. nov. to formally recognize clades Fr3 and H as genera in the family Symbiodiniaceae (Dinophyceae). J Phycology 56(4), 923–940. https://doi.org/10.1111/jpy.12999
49. MacVittie S, Doroodian S, Alberto A, Sogin M (2024) Microbiome depletion and recovery in the sea anemone, *Exaiptasia diaphana*, following antibiotic exposure. Msystems 9(6), e01342–23. https://doi.org/10.1128/msystems.01342-23
50. McCauley M, Montesanto F, Bedgood SA, Hartman LM, van Oppen MJH, Goulet TL (2025) Manipulation of the Symbiodiniaceae microbiome confers multigenerational impacts on symbioses and reproductive ecology of its *Exaiptasia diaphana* host. *The ISME Journal* 19, wraf189. https://doi.org/10.1093/ismejo/wraf189
51. Minh BQ, Schmidt HA, Chernomor O, Schrempf D, Woodhams MD, Von Haeseler A, Lanfear R (2020) IQ-TREE 2: new models and efficient methods for phylogenetic inference in the genomic era. Mol Biol Evol, 37(5), 1530–1534. https://doi.org/10.1093/molbev/msaa015
52. Morejón-Arrojo RD, Lüskow F, Pakhomov EA, Guendulain-García SD, Dáttilo W, Rodríguez-Viera L, Hoeksema BW (2025) A review of benthic cnidarians as underappreciated predators in the gelatinous ocean. Mar Biol 172, 4625. https://doi.org/10.1007/s00227-025-04625-4
53. Moya-Hernández N, Moya IM (2026) From bleaching to restoration: mechanisms of mutualism recovery in *Exaiptasia* and implications for coral symbiosis. Front Mar Sci 13, 1805924. https://doi.org/10.3389/fmars.2026.1805924
54. Murray AE, Rack FR, Zook R, Williams MJM, Higham ML, Broe M, Kaufmann RS, Daly M (2016) Microbiome composition and diversity of the ice-dwelling sea anemone, *Edwardsiella andrillae*. Integr Comp Biol 56(4), 542–555. https://doi.org/10.1093/icb/icw095
55. Parkinson JE, Coffroth MA, LaJeunesse TC (2015) New species of Clade B *Symbiodinium* (Dinophyceae) from the greater Caribbean belong to different functional guilds: *S. aenigmaticum* sp. nov, *S. antillogorgium* sp. nov, *S. endomadracis* sp. nov, and *S. pseudominutum* sp. nov. J Phycol 51(5), 850–858. https://doi.org/10.1111/jpy.12340
56. Parkinson JE, Peixoto RS, Voolstra CR (2025) Symbiodiniaceae. Coral Reef Microbiome, 17–46. Springer. https://doi.org/10.1007/978-3-031-76692-3_2
57. Pochon X, Putnam HM, Burki F, Gates RD (2012) Identifying and characterizing alternative molecular markers for the symbiotic and free-living dinoflagellate genus *Symbiodinium*. PloS one 7(1), e29816. https://doi.org/10.1371/journal.pone.0029816
58. Rodríguez E, Barbeitos MS, Brugler MR, Crowley LM, Grajales A, Gusmão L, Häussermann V, Reft A, Daly M (2014) Hidden among sea anemones: the first comprehensive phylogenetic reconstruction of the order Actiniaria (Cnidaria, Anthozoa, Hexacorallia) reveals a novel group of hexacorals. PLoS One 9:e96998. https://doi.org/10.1371/journal.pone.0096998
59. Ruggeri M, Million WC, Hamilton L, Kenkel CD (2024) Microhabitat acclimatization alters sea anemone–algal symbiosis and thermal tolerance across the intertidal zone. Ecology 105, e4388. https://doi.org/10.1002/ecy.4388
60. Schloss PD, Westcott SL, Ryabin T, Hall JR, Hartmann M, Hollister EB, Lesniewski RA, Oakley BB, Parks DH, Robinson CJ, Sahl JW, Stres B, Thallinger GG, Van Horn DJ, Weber CF (2009) Introducing mothur: Open-source, platform-independent, community-supported software for describing and comparing microbial communities. Appl Environ Microbiol 75(23), 7537–7541. https://doi.org/10.1128/AEM.01541-09
61. Stöver BC, Müller KF. (2010) TreeGraph 2: combining and visualizing evidence from different phylogenetic analyses. BMC Bioinformatics 11(1), 7. https://doi.org/10.1186/1471-2105-11-7

62. Sun J, Hamel JF, Shikon V, Cossignani EF, Mercier A (2021) Trophic ecology, diet and feeding behaviour of three bathyal sea anemones (Actiniaria: Cnidaria) in the Northwest Atlantic. Deep-Sea Res I: Oceanogr Res Pap 179, 103678. https://doi.org/10.1016/j.dsr.2021.103678
63. Sydnor JR, Lacy SB, Bachvaroff TR (2023) Changes in the microbiome of the sea anemone *Exaiptasia diaphana* during bleaching from short-term thermal elevation. Front Mar Sci 10, 1130964. https://doi.org/10.3389/fmars.2023.1130964
64. Targino AKG, Gomes PB (2020) Distribution of sea anemones in the Southwest Atlantic: biogeographical patterns and environmental drivers. Mar Biodivers 50, 80. https://doi.org/10.1007/s12526-020-01099-z
65. Zapata F, Goetz FE, Smith SA, Howison M, Siebert S, Church SH, Sanders SM, Ames CL, McFadden CS, France SC, Daly M, Collins AG, Haddock SHD, Dunn CW, Cartwright P (2015) Phylogenomic analyses support traditional relationships within Cnidaria. *PLoS ONE* 10(10), e0139068. https://doi.org/10.1371/journal.pone.0139068

## Figures

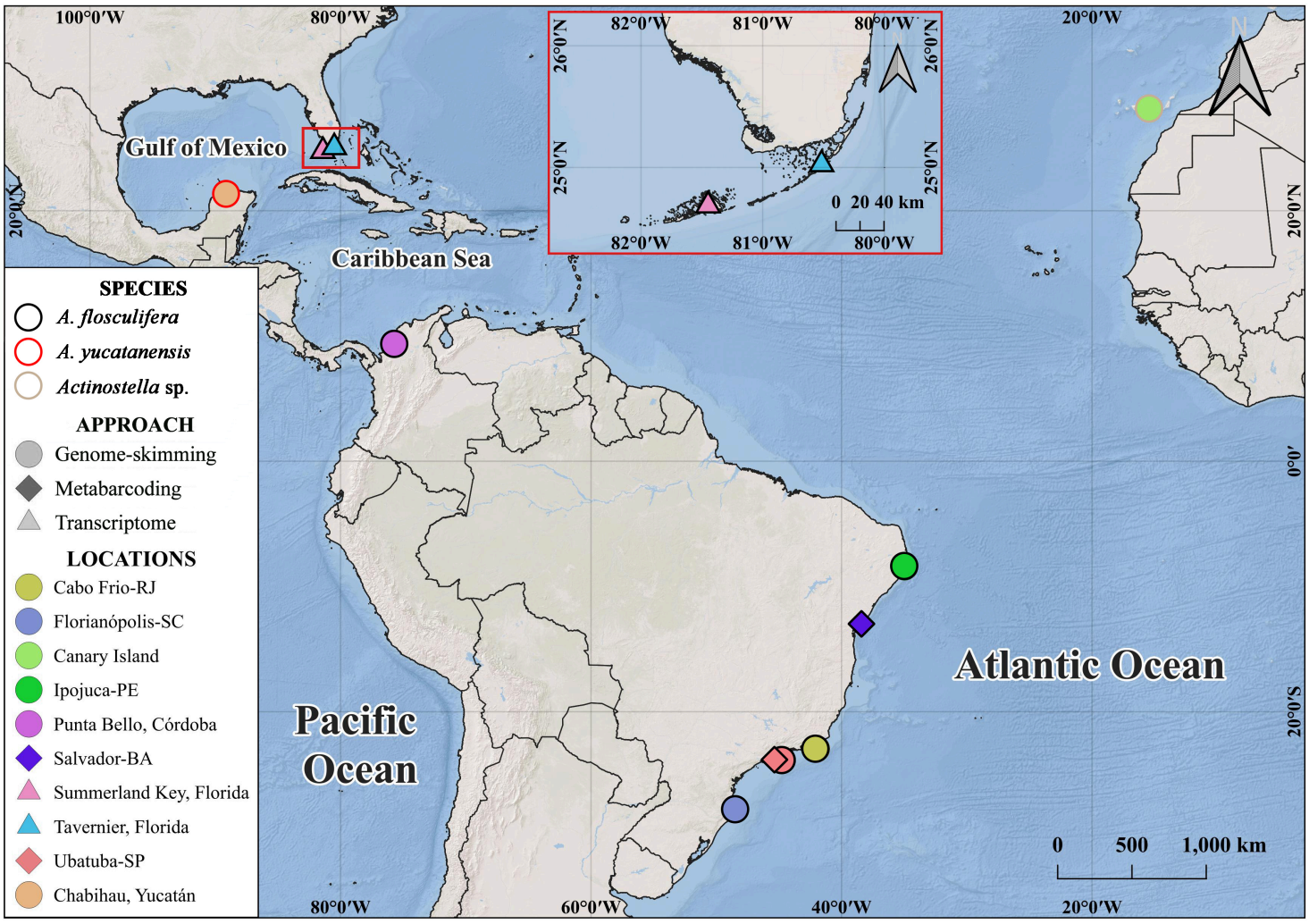
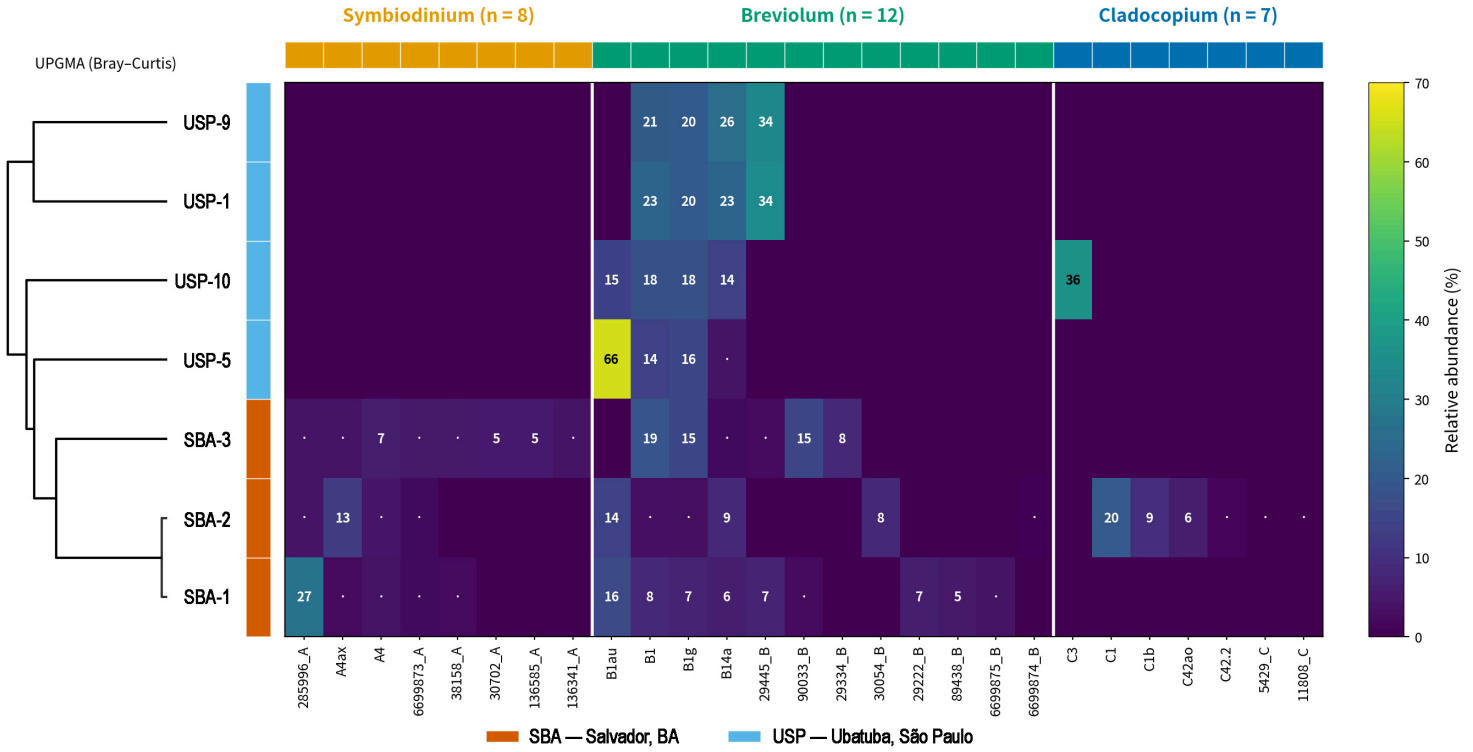



**Figure 1**

Map of sampling localities and sequencing approaches used to characterize endosymbiotic communities associated with *Actinostella* spp. Colors denote localities, species, and symbols indicate the sequencing strategy (genome-skimming, metabarcoding, and transcriptomics).




## Figure 2

Heatmap of the 27 ITS2 type profiles (columns) recovered using the SymPortal analytical framework (Hume et al. 2019) on metabarcoding data from seven *Actinostella flosculifera* specimens (rows). Cell colour intensity is proportional to the post-MED relative abundance of each ITS2 profile in each specimen (deep blue = absent; yellow = 70% of reads); numerical values are shown for cells with ≥ 5% abundance, and a dot indicates non-zero abundance below 5%. ITS2 profiles are grouped by Symbiodiniaceae genus (top colour bar): *Symbiodinium*(Clade A, orange, N = 8 profiles); *Breviolum* (Clade B, green, N = 12 profiles); *Cladocopium* (Clade C, blue, N = 7 profiles). Within each genus, profiles are ordered by cumulative abundance across all specimens. Sample-level UPGMA dendrogram (left) is based on the Bray–Curtis dissimilarity matrix computed from the full 7 × 27 abundance matrix. The vertical bar to the left of the heatmap indicates the biogeographic origin of each specimen (orange = SBA — Salvador, BA; blue = USP — Ubatuba, SP). The dendrogram resolves two well-supported clusters that perfectly recover the regional split, a Ubatuba cluster (top, four USP specimens) and a Salvador cluster (bottom, three SBA specimens), while internal sub-structure reveals microhabitat-driven sub-generic turnover within each region.




**Figure 3**

Distribution of assembled contigs along clade-specific Symbiodiniaceae ribosomal reference sequences following the mapping and assembly of genome-skimming and transcriptomic reads from *Actinostella* spp. Horizontal lines represent individual contigs aligned to the reference sequences for *Symbiodinium* and *Breviolum*. Colored bars indicate the annotated ribosomal regions (18S, ITS1, 5.8S, ITS2, and 28S).

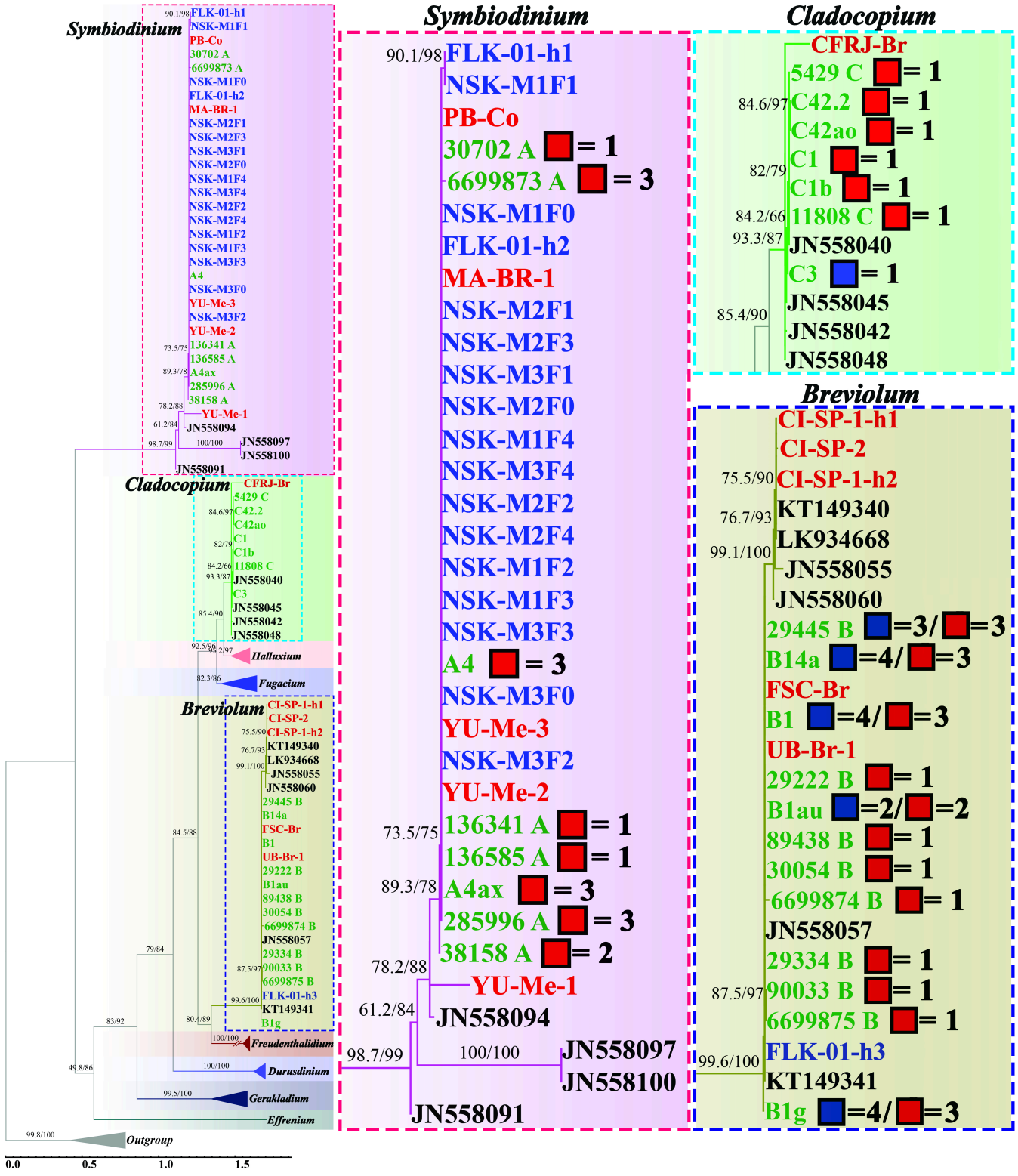



**Figure 4**

Maximum-likelihood phylogeny based on ITS2 sequences of Symbiodiniaceae associated with *Actinostella*spp., recovered through transcriptomic (blue terminals), genome-skimming (red terminals), and metabarcoding (green terminals) approaches. Black terminals represent reference sequences retrieved from GenBank. The left panel shows the complete phylogeny, whereas the center and right panels are enlarged views of the highlighted regions corresponding to *Symbiodinium* and *Breviolum–Cladocopium*, respectively. Node support values are shown as SH-aLRT/UFBoot (%).

Colored squares indicate the number of samples containing each ITS2 sequence in SymPortal profiles from Salvador, Bahia (SBA; red) and Ubatuba, São Paulo (USP; blue).

## Supplementary Files

This is a list of supplementary files associated with this preprint. Click to download.

- SupplementaryTableS14.xlsx